

# Stable Expression of FoxA1 Promotes Pluripotent P19 Embryonal Carcinoma Cells to Be Neural Stem-Like Cells

DIFEI DONG,<sup>1</sup> LEI MENG,<sup>1</sup> QIQI YU, GUIXIANG TAN, MIAO DING, AND YONGJUN TAN

*State Key Laboratory of Chemo/Biosensing and Chemometrics, College of Biology, Hunan University, Changsha, Hunan, China*

FoxA1 belongs to the fork head/winged-helix transcription factor family and participates in stimulating neuronal differentiation of pluripotent stem cells at early stages. To explore the biological roles of FoxA1 during this process, the stable expression of a GFP-FoxA1 fusion protein was established in P19 pluripotent embryonal carcinoma cells. Although they still express pluripotency-related transcription factors such as Oct4, Nanog, and Sox2, the generated P19 GFPFoxA1 cells exhibited a decreased activity of alkaline phosphatase and an increased expression of SSEA-3 compared with P19 cells. Elevated levels of nestin expression and prominin-1<sup>+</sup> populations were observed in P19 GFPFoxA1 cells, implicating that the stable expression of FoxA1 promoted P19 cells to gain partial characteristics of neural stem cells. Furthermore, the promoter of nestin was confirmed to be bound and activated by FoxA1 directly. The expression of neuron-specific marker tubulin  $\beta$ III also existed in P19 GFPFoxA1 cells. P19 GFPFoxA1 cells showed an earlier onset of differentiation during RA-induced neuronal differentiation, evidenced by a more rapid change on the Nanog decrease and the tubulin  $\beta$ III increase. Thus, overexpression of FoxA1 alone may promote pluripotent P19 cells to become neural stem-like cells.

Key words: FoxA1 transcription factor; Pluripotent P19 embryonal carcinoma (EC) cells; Nestin; Retinoic acid-induced neuronal differentiation; Stable cell line

## INTRODUCTION

Transcription factor FoxA1 belongs to the fork head/winged-helix family of transcription factors that play important roles in cellular proliferation and differentiation during embryonic development (9,13,14, 17). FoxA1 participates in the early development of central nervous system and endoderm-derived organs like liver and pancreas, evidenced by its expression initiating during gastrulation of mouse embryogenesis in notochord, ventral floor plate of neural tube, and gut endoderm, and spreading to midbrain and spinal cord regions and to liver primordium (2,23,29, 30). It possesses multiple functions in different adult organs because its expression in the adult includes tissues derived from endoderm, mesoderm, and

neurectoderm (3). The expression pattern of FoxA1 in developing neural tube and adult brain structures implicates its important roles in neurogenesis and brain functions. This is supported by a recent discovery in which FoxA1 was found to regulate multiple phases of midbrain dopaminergic neuron development by stimulating expression of multiple neural differentiation-related genes at different stages of the neuronal differentiation (8).

Pluripotent stem cells are undifferentiated cells that can give rise to several lineages of differentiated cell types (38). Among the well-established pluripotent cells such as embryonic stem cells (ESCs) and embryonic germ cells (EGCs), embryonal carcinoma cells (ECCs) are derived from teratocarcinomas and have been well characterized as pluripotent cell lines

<sup>1</sup>These authors provided equal contribution to this study.

Address correspondence to Yongjun Tan, State Key Laboratory of Chemo/Biosensing and Chemometrics, College of Biology, Hunan University, Changsha, Hunan 410082, China. Tel/Fax: (86) 731-8882-3211; E-mail: [yjtan@hnu.edu.cn](mailto:yjtan@hnu.edu.cn)

that can be maintained as undifferentiated cells and induced under controlled conditions to differentiate in vitro to any cell type of all three germ layers (19). The mouse P19 EC cell line was derived from a teratocarcinoma in C3H/He mice, produced by grafting an embryo at 7 days of gestation to testes of an adult male mouse (21). The cells contain a normal karyotype, predicting that the cells do not possess any gross genetic abnormalities. When injected into mouse blastocysts, P19 cells differentiate into a broad range of cell types in the resulting chimeras (28). Like ES cells, P19 cells express pluripotent marker genes such as Oct4, Nanog, and Sox2 and possess high activity of alkaline phosphatase, and teratomas formed by P19 cells in a nude mouse contains all three embryonic germ layers (37). P19 cells can differentiate in vitro into derivatives of all three germ layers depending on chemical treatment and growth conditions. For example, P19 cell aggregates (embryoid bodies) differentiate to cardiac and skeletal muscle when treated with dimethyl sulfoxide (7,20), or neuronal and glial cells with retinoic acid (RA) treatment (12,20).

The model of RA-induced P19 cell neuronal differentiation has been widely used for molecular analysis of neuronal induction and differentiation (15,24,26,31,35,36). The temporal patterns of gene expression during RA-induced P19 cell neuronal differentiation display three phases: the initial primary response phase (0–24 h following RA treatment), the neural differentiation phase (1–3 days following RA treatment), and the terminal differentiation phase (5–6 days following RA treatment). FoxA1 is induced within 6 h and peaks at 1 day during RA-induced P19 cell neuronal differentiation (10), and is one of the primary targets of RA action through a RA-responsive element (RARE) in its promoter (11). Our recent data have demonstrated that adenovirus-mediated transient elevation of FoxA1 promotes pluripotent P19 cells to become neural stem-like cells through its direct stimulation on the expression of sonic hedgehog (Shh). Knockdown of FoxA1 prevents the induction of Shh and nestin during P19 cell neuronal differentiation. Elevated levels of FoxA1 also enhance the overall neuronal differentiation, evidenced by increased populations of neurons at the late time point of RA-induced neuronal differentiation (34).

In this study, we intend to further explore the biological roles of FoxA1 during neuronal differentiation. We have established P19 cell-derived cell lines that stably express a GFPFoxA1 fusion protein. We have found that the stable expression of GFPFoxA1 in P19 cells results in a decreased activity of alkaline phosphatase and an increased expression of SSEA-3.

Furthermore, elevated levels of nestin expression and prominin-1<sup>+</sup> populations are observed in P19 GFP-FoxA1 cells, implicating that the obtained cell lines gain partial characteristics of neural stem cells. We have confirmed that the promoter of nestin is bound and activated by FoxA1 directly. We have demonstrated that P19 GFPFoxA1 cells show an earlier onset of differentiation during RA-induced neuronal differentiation, evidenced by a more rapid change on the Nanog decrease and the tubulin  $\beta$ III increase. Thus, FoxA1 may be one of the major factors that promote pluripotent P19 cells to become neural stem-like cells.

## MATERIALS AND METHODS

### *Cell Culture and RA-Induced Neural Differentiation*

The P19 EC cells were maintained in DMEM containing 7.5% calf serum (Gibco), 2.5% fetal bovine serum (Gibco), and 0.5% penicillin streptomycin (Gibco) at 37°C in 5% CO<sub>2</sub>. For neural differentiation, P19 cell aggregates were formed by placing 3 × 10<sup>6</sup> P19 cells in a 100-mm bacterial grade dish (petri dish; Falcon) with addition of 5 × 10<sup>-7</sup> M all-*trans* RA (Sigma) for 4 days.

### *Generation of FoxA1-Expressed P19 Cell Lines*

The cDNA of rat FoxA1 was PCR amplified by pfu DNA polymerase (Fermentas) from the template of rat HNF3 $\alpha$  cDNA (32), with the following restriction site tagging sense (S) and antisense (AS) primers: *EcoRI*-rFoxA1-S, 5'-CCG GAA TTC CGG ATG TTA GGG ACT GTG AAG-3' and *BamHI*-rFoxA1-AS, 5'-CCC AAG CTT GGG CTA GGA AGT ATT TAG CAC-3'. The *EcoRI/BamHI* fragment of rat FoxA1 PCR products was inserted into the *EcoRI/BamHI* site of a pEGFP-C2 vector (Clontech #6083-1). The expression vector of pCMVp-EGFP-rFoxA1 was transfected into P19 cells with Lipofectamine 2000 (Invitrogen) and stable transfectants were obtained following the selection with 500  $\mu$ g/ml of G418 (Invitrogen) for 14 days. The individual clone of GFP-FoxA1-expressed cells was established by limiting dilutions.

### *Reverse Transcription Polymerase Chain Reaction (RT-PCR)*

For RT-PCR, the cDNAs were synthesized using RevertAid<sup>TM</sup> First Strand cDNA Synthesis Kits (Fermentas) with total RNA as templates. PCR amplification was performed with Taq DNA polymerase (Promega) with following sense (S) and antisense (AS) primers, annealing temperature ( $T_a$ ), and

number of PCR cycles ( $N$ ): mNanog-S, 5'-GAG ACA GAA GGA CCA GGA GT-3' and mNanog-AS, 5'-GGA CTC CAA GGA CAA GCA AG-3' ( $T_a$ : 58°C,  $N$ : 30); mOct4-S, 5'-CAC TTT GGC ACC CCA GGC TA-3' and mOct4-AS, 5'-GCC TTG GCT CAC AGC ATC CC-3' ( $T_a$ : 58°C,  $N$ : 30); mSox2-S, 5'-TGA CCA GCT CGC AGA CCT AC-3' and mSox2-AS, 5'-GGA GGA AGA GGT AAC CAC GG-3' ( $T_a$ : 58°C,  $N$ : 30); mCyclophilin-S, 5'-GGC AAA TGC TGG ACC AAA CAC-3' and mCyclophilin-AS, 5'-TTC CTG GAC CCA AAA CGC TC-3' ( $T_a$ : 58°C,  $N$ : 26); rFoxA1-S, 5'-TAC GCT CCG TCC AAT CTG GG-3' and rFoxA1-AS, 5'-TGA GTG GCG AAT GGA GTT CTG-3' ( $T_a$ : 63.6°C,  $N$ : 30); mFoxA1-S, 5'-AGA CAT TCA AGC GCA GCT ACC-3' and mFoxA1-AS, 5'-GGG TCC TTG CGA CTT TCT G-3' ( $T_a$ : 57.5°C,  $N$ : 30); mNestin-S, 5'-TCG ATG ACC TGG AGG GAC AAC-3' and mNestin-AS, 5'-AAA TGC CTT GGG TCC TCT AGC C-3' ( $T_a$ : 63°C,  $N$ : 30); mTubulin  $\beta$ III-S, 5'-GAT GAT GAC GAG GAA TCG GAA G-3' and mTubulin  $\beta$ III-AS, 5'-AGA GGT GGC TAA AAT GGG GAG G-3' ( $T_a$ : 58.2°C,  $N$ : 28); mShh-S, 5'-CAA TCT GCA ACG GAA GCG AG-3' and mShh-AS, 5'-GTG CGC TTT CCC ATC AGT TCC-3' ( $T_a$ : 64°C,  $N$ : 35).

#### Western Blotting, Immunostaining, and Flow Cytometry

To measure protein levels, Western blot analysis with antibodies against proteins of interest was performed as described previously (33). The following antibodies and dilutions were used for Western blotting: rabbit anti-FoxA1 (1:2,000; abcam ab23738), rabbit anti-Nanog (1:2,500; Chemicon AB9220), rabbit anti-Oct4 (1:1500; Chemicon AB3209), rabbit anti-Sox2 (1:1500; abcam AB59776), rabbit anti-nes- tin (1:2500; Milipore AB5922), mouse anti-tubulin  $\beta$ III (1:1,000; Chemicon MAB1637), mouse anti-GFP (1:1000, Milipore MAB3580), and mouse anti- $\beta$ -actin (1:20,000; Sigma AC-15).

Immunostaining of selected proteins was performed as described previously (34). The following antibodies and dilutions were used for immunostaining: rabbit anti-nes- tin (1:100; Milipore AB5922) and mouse anti-tubulin  $\beta$ III (1:100; Chemicon MAB1637).

Flow cytometry of selected markers was performed as described previously (37). The following antibodies were used for flow cytometry: SSEA-3-PE antibody (eBioscience 12-8833-71) and prominin-1-PE antibody (Miltenyi Biotec 130-092-334).

#### Alkaline Phosphatase Staining

Cells were fixed with 50% acetone and 50% methanol at room temperature for 2 min and stained using

an alkaline phosphatase (ALP) staining kit (Vector Laboratories Burlingame) according to a standard protocol.

#### Chromatin Immunoprecipitation (ChIP) Assays and Cotransfection Assays

ChIP assays were performed as previously described (34). For immunoprecipitation, 2  $\mu$ g of rabbit anti-FoxA1 (abcam ab23738) or rabbit control IgG anti-cdc25B (Santa Cruz SC-326) was used. The ChIP DNA sample or 5% total input was used in PCR with the following primers: mNestin promoter -4064 bp forward: 5'-AAC AGC AAC AAC CAC AAC ACT GC-3' and mNestin promoter -3919 bp backward: 5'-GGA ACC CTC TCT CAA CCT TTG G-3' ( $T_a$ : 60°C,  $N$ : 35), mNestin promoter -2010 bp forward: 5'-TCA GAG GCT TTG ATG TCC CTG G-3' and mNestin promoter -1855 bp backward: 5'-ACA GAT TGG CAT TCT CAG CAC TG-3' ( $T_a$ : 60°C,  $N$ : 35).

For cotransfection assays, the mouse -372 to +197 bp nestin promoter region was PCR amplified from mouse genomic DNA with the following primers: mNestin -372 *Hind*III 5'-CCG AAG CTT TCC GTT TTT CCA ACA GTT CAC G-3' and mNestin +197 *Hind*III 5'-CCG AAG CTT TGA GCA GCT GGT TCT GCT CCT C-3', and cloned into the corresponding *Hind*III site of the pGL3 basic Luciferase vector (Promega). The mouse nestin promoter -4179 to -3919 region was PCR amplified from mouse genomic DNA with the following primers: mNestin -4179 *Xho*I 5'-CCG CTC TAG TGA CAC CCT CTT CTG GCA CAT C-3' and mNestin -3919 *Hind*III 5'-CCG AAG CTT GGA ACC CTC TCT CAA CCT TTG G-3', and cloned into the corresponding *Xho*I/*Hind*III sites of pGL3-Nestin-372bp-Promoter. P19 cells were transfected with 200 ng of either CMV-FoxA1 cDNA or CMV empty expression vectors, 1,600 ng of the Luciferase reporter constructs containing different mouse nestin promoter regions, and 25 ng of pRL-CMV loading control Luciferase reporter plasmid (Promega) by Lipofectamine 2000 reagent (Invitrogen). Protein extracts were prepared from transfected P19 cells at 24 h following DNA transfection and the Dual-Luciferase Assay System (Promega) was used to measure Luciferase enzyme activity following the manufacturer's instructions.

#### Statistical Analysis

We used Microsoft Excel Program to calculate SD and statistically significant differences between samples with Student's *t*-test. The asterisks in each graph indicate statistically significant changes with *p*-values calculated by Student's *t*-test: \**p* < 0.05, \*\**p*  $\leq$  0.01,

and  $***p \leq 0.001$ . Values of  $p < 0.05$  were considered statistically significant.

## RESULTS AND DISCUSSION

### *The Construction of P19 Cells That Stably Express a Functional GFPFoxA1 Fusion Protein*

The aggregated P19 cells were differentiated to neural cells by RA treatment (12,20) and a transient elevation of FoxA1 alone could promote the cells to be neural stem-like cells through FoxA1's direct stimulation on the expression of Shh (34). To further explore the functions of FoxA1 during neuronal differentiation, we stably expressed the protein of FoxA1 in P19 cells. A plasmid vector that contained a CMV promoter-driven GFP-rat FoxA1 cDNA expression cassette was transfected to P19 cells. After the G418 selection for 2 weeks, P19 cell-derived cell lines that stably expressed a GFP-rat FoxA1 fusion protein were established and named as P19 GFP-FoxA1 cells. Three individual clones (clone 1, 2, and 3) were analyzed by RT-PCR with the designed primers specific to GFP-rat FoxA1 fusion cDNA to confirm the expression of exogenous GFPFoxA1 mRNAs in P19 GFPFoxA1 cells (Fig. 1A). The clone

1 cells were chosen to measure the expression of GFPFoxA1 fusion protein, which was visualized by fluorescence microscopy (Fig. 1B). The analysis of flow cytometry confirmed that more than 95% cells of clone 1 were GFP positive compared to P19 cells (Fig. 1C). The Western blotting results of the clone 1 cells showed that the molecular weight of the expressed GFPFoxA1 fusion protein was close to the theoretically calculated value (Fig. 1D). We transfected a reporter plasmid, in which the luciferase reporter gene was driven by a promoter containing 6 $\times$  FoxA binding sites (TTTGTTTGTGTTG) from Cdx2 promoter (27), to the clone 1 cells and confirmed the transcriptional activity of GFPFoxA1 fusion protein (Fig. 1E). Therefore, we established P19-derived cell lines that stably expressed a functional GFPFoxA1 fusion protein.

### *The Decreased Activity of Alkaline Phosphatase and Increased Expression of SSEA-3 in P19 GFPFoxA1 Cells*

P19 cells are pluripotent stem cells, evidenced by high expression levels of pluripotency-related genes such as Oct4, Nanog, and Sox2, and the formation of three germ layer-containing teratomas upon subcutaneous

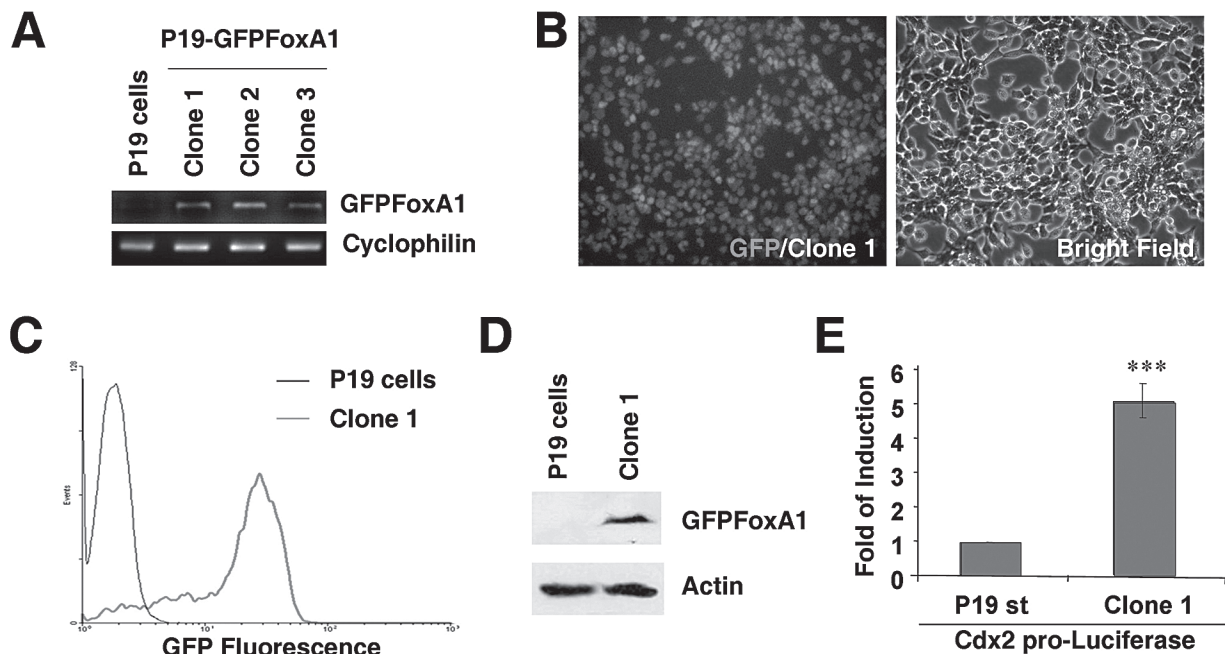


Figure 1. P19 EC cells that stably express a functional GFPFoxA1 fusion protein. (A) Stable expression of GFPFoxA1 in P19 cells. GFPFoxA1-expressing P19 cell lines were established according to procedures detailed in Materials and Methods. Total RNA samples were isolated from P19 cells and three individual clones (clone 1, 2, and 3) of P19 GFPFoxA1 cells, and the mRNA levels of GFPFoxA1 and cyclophilin were measured by RT-PCR Assays. (B–E) The established P19 GFPFoxA1 cells express a functional fusion protein. The clone 1 cells were chosen to measure the expression of GFPFoxA1 fusion protein by fluorescence microscopy (B), flow cytometry (C), and Western blotting (D). The transcriptional activity of GFPFoxA1 fusion protein was confirmed by the activation of FoxA1 binding sites containing promoter (Cdx2 promoter) in clone 1 cells (E).

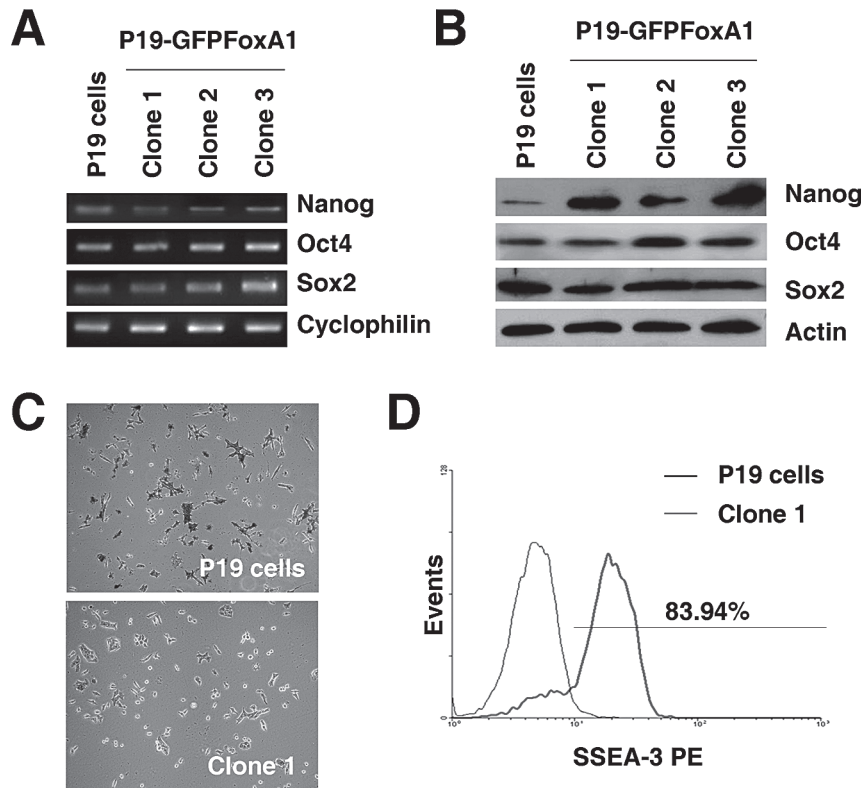


Figure 2. The stable expression of GFPFoxA1 in P19 cells correlates with decreased activity of alkaline phosphatase and increased expression of SSEA-3. (A, B) P19 GFPFoxA1 cells normally express pluripotency-related transcription factors such as Oct4, Nanog, and Sox2. Total RNA or proteins samples were isolated from P19 cells and clone 1, 2, and 3 of P19 GFPFoxA1 cells. The mRNA or protein levels of Oct4, Nanog, and Sox2 were measured by RT-PCR assays (A) or Western blotting (B), respectively. Cyclophilin or  $\beta$ -actin was used as the loading control. (C) P19 cells and the clone 1 cells were stained for alkaline phosphatase. (D) GFPFoxA1 stable expression resulted in significant increase of SSEA-3 in P19 cells. Flow cytometry was used to measure cell populations of SSEA-3 in P19 cells and the clone 1 cells. P19 cells were used as negative control cells.

inoculation into nude mice (37). We measured the expression of Oct4, Nanog, and Sox2 in P19 GFPFoxA1 cells, and found that the cells normally expressed the mRNAs (Fig. 2A) and proteins (Fig. 2B) of these transcription factors. On the other hand, even though both P19 and P19 GFPFoxA1 cells possessed a similar proliferation rate (Fig. 1S; supplement figures available from [http://bio.hnu.cn/index.php?option=com\\_content&view=article&id=131:2010-11-16-12-45-48&catid=46:2010-07-19-05-57-39&Itemid=123](http://bio.hnu.cn/index.php?option=com_content&view=article&id=131:2010-11-16-12-45-48&catid=46:2010-07-19-05-57-39&Itemid=123)), we noticed that P19 GFPFoxA1 cells showed a decreased activity of alkaline phosphatase (Fig. 2C), implicating that the cells lost partial characteristics of pluripotent stem cells. This idea was further supported by the analysis of the SSEA-3 expression of P19 GFPFoxA1 cells with flow cytometry. The cell surface antigen SSEA-3 did not express in mouse pluripotent stem cells but was upregulated following differentiation (1,5). We found that the 83.94% population of P19 GFPFoxA1 cells was SSEA-3 positive compared with that of P19 cells (Fig. 2D), suggesting

the differences between the P19 GFPFoxA1 cells and parental P19 EC cells.

#### *P19 GFPFoxA1 Cells Showed Elevated Levels of Nestin Expression and Prominin-1<sup>+</sup> Populations*

Adenovirus-mediated transient elevation of FoxA1 promotes pluripotent P19 cells to become neural stem-like cells through the direct stimulation on the Shh expression and enhances the overall neuronal differentiation (34). To further characterize the phenotype of P19 GFPFoxA1 cells, we measured the expression of neural stem cell marker nestin (18) in these cells. The mRNA levels were measured by RT-PCR assays with the samples from P19 cells and clone 1, 2, and 3 of P19 GFPFoxA1 cells. The expression of Shh was increased in the clones of P19 GFPFoxA1 cells as expected and a dramatic increase of nestin mRNAs was also found in these clones (Fig. 3A). The elevated expression of nestin in P19 GFPFoxA1 cells was confirmed by Western blotting

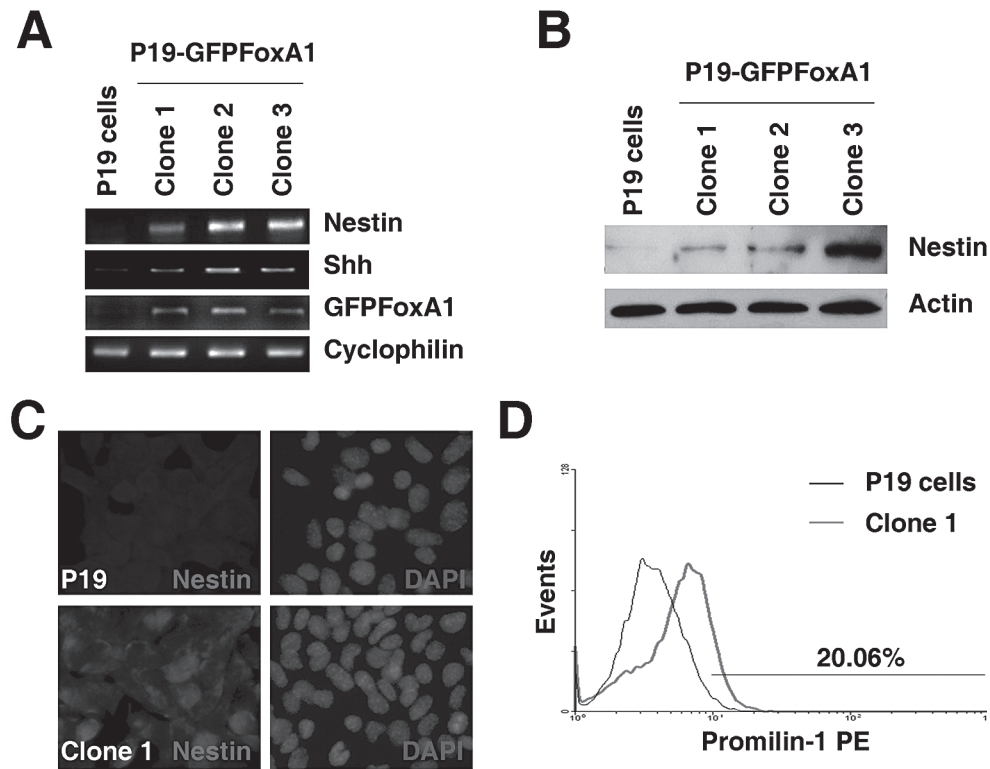


Figure 3. Elevated levels of nestin expression and prominin-1<sup>+</sup> populations in P19 GFPFoxA1 cells. (A–C) P19 GFPFoxA1 cells express neural stem cell marker nestin. Total RNA or protein samples were isolated from P19 cells and clone 1, 2, and 3 of P19 GFPFoxA1 cells. The mRNA levels of nestin, Shh, GFPFoxA1, and cyclophilin were measured by RT-PCR assays (A). The protein levels of nestin and  $\beta$ -actin were measured by Western blotting (B). Immunostaining of P19 cells or the clone 1 cells was performed with nestin antibody (C). (D) P19 GFPFoxA1 cells contained populations of neural stem cells (prominin-1<sup>+</sup> cells). Flow cytometry was used to measure cell populations of prominin-1<sup>+</sup> cells in the clone 1 cells, compared to P19 cells.

and immunostaining with nestin antibody (Fig. 3B, C). This finding suggested that the stable expression of GFPFoxA1 promoted P19 cells to gain partial characteristics of neural stem cells. This idea was further supported by the flow cytometry analysis, in which P19 GFPFoxA1 cells was found to contained increased cell populations positive with neural stem cell-surface marker prominin-1 (homolog of human CD133) compared to P19 cells (Fig. 3D).

#### *FoxA1 Binds to and Stimulates Nestin Promoter*

To test whether FoxA1 was one of the regulators of nestin transcription, we scanned  $-5$  kb promoter region of mouse nestin gene with the FoxA1 DNA binding consensus sequence, and found multiple tandem FoxA1 putative binding sites at the regions of  $-4085$  to  $-4073$  bp,  $-3439$  to  $-3427$  bp, and  $-1761$  to  $-1748$  bp in the nestin promoter (Fig. 4A). We used chromatin immunoprecipitation (ChIP) assays to determine the nestin promoter regions that mediate FoxA1 binding to endogenous nestin promoter at physiological conditions. The chromatin of P19 cells, RA-induced (2d) P19 cells, or AdFoxA1-infected

(2d) P19 cells (34) was cross-linked, sonicated to DNA fragments of 500–1000 nucleotides in length, and then immunoprecipitated with either rabbit FoxA1 antibody or rabbit control IgG (anti-cdc25B). The amount of promoter DNA associated with the IP chromatin was quantitated by RT-PCR with primers specific to nestin promoter region  $-4064$  to  $-3919$  bp or  $-2010$  to  $-1855$  bp. Compared to the P19 cell samples that showed no FoxA1 specific binding, RA-treated or AdFoxA1-infected samples showed obvious binding activities of FoxA1 on the nestin promoter region around  $-4$  kb but not the  $-2$  kb region (Fig. 4B). These results confirmed that FoxA1 bound directly to endogenous nestin promoter at  $-4$  kb upstream region during RA-induced differentiation. To test whether FoxA1 activates nestin promoter, luciferase reporter plasmids with different length of mouse nestin promoter regions were constructed and transfected into P19 cells with the CMV-FoxA1 expression vector or a CMV empty expression vector. Luciferase enzyme activity was analyzed following transfection. Cotransfection of FoxA1 expression vector caused a significant increase in  $-4$  kb nestin promoter activity (Fig. 4C).

*P19 GFPFoxA1 Cells Showed an Earlier Onset of Neuronal Differentiation Through RA Treatment*

P19 cells are known to differentiate into neuronal cells by RA treatment and cellular aggregation (12,20). Surprisingly, we found a noticeable increase of neuron-specific marker tubulin  $\beta$ III in P19 GFPFoxA1 cells at the mRNA levels measured by RT-PCR assays (Fig. 5A). The elevated expression of tubulin  $\beta$ III in P19 GFPFoxA1 cells was confirmed by immunostaining (Fig. 5B) and Western blotting (Fig. 5C) with tubulin  $\beta$ III antibody. To determine whether P19 GFPFoxA1 cells maintain the ability to differentiate to neuronal cells, the cells were

cultured in accordance with standard procedures required for neuronal differentiation to occur. P19 GFPFoxA1 cells were able to form cell aggregates in bacterial grade dishes during RA stimulation, although the P19 GFPFoxA1 cell aggregates were observed morphologically to be loose and irregular compared with that of P19 cells (Figs. 2S, 3S, A; supplement figures available from [http://bio.hnu.cn/index.php?option=com\\_content&view=article&id=131:2010-11-16-12-45-48&catid=46:2010-07-19-05-57-39&Itemid=123](http://bio.hnu.cn/index.php?option=com_content&view=article&id=131:2010-11-16-12-45-48&catid=46:2010-07-19-05-57-39&Itemid=123)). The RA-initiated neuronal differentiation of P19 GFPFoxA1 cells progressed faster than that of P19 cells, evidenced by a more rapid decrease of Nanog, which is one of the critical transcription factors that

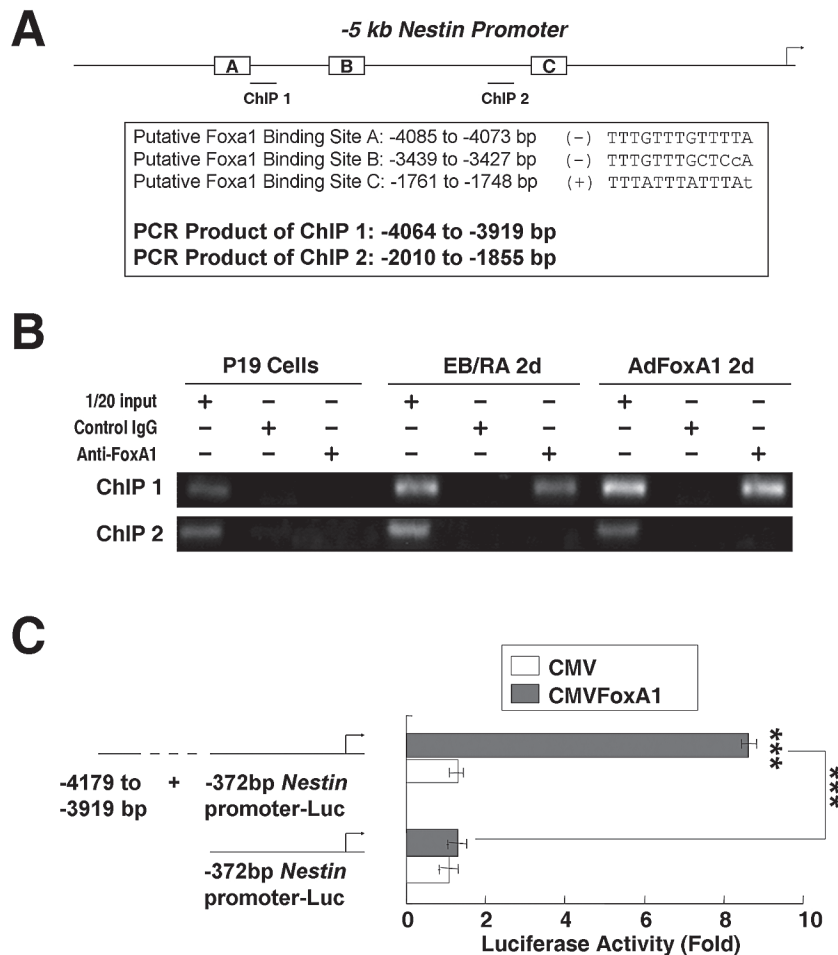


Figure 4. FoxA1 binds to and stimulates nestin promoter. (A) The predicted positions of putative FoxA1 binding sites in  $-5$  kb mouse nestin promoter by gene sequence analysis and the positions of primers designed for ChIP assays. (B) FoxA1 bound to endogenous nestin promoter. ChIP assays were used to show direct binding of FoxA1 to endogenous nestin promoter regions. The chromatin of P19 cells, RA-induced (2d) P19 cells, or AdFoxA1-infected (2d) P19 cells was cross-linked, sonicated, and immunoprecipitated with either FoxA1 antiserum or rabbit serum (control) and the amount of promoter DNA associated with the IP chromatin was quantitated by RT-PCR with primers specific to different nestin promoter regions. The predicted size of the PCR product was 145 bp (ChIP1) or 155 bp (ChIP2). (C) The endogenous FoxA1 binding sites in  $-4$  kb region of nestin promoter mediated the transcription activity of FoxA1. The nestin promoters with different length were constructed into luciferase reporter plasmid. The different reporter plasmid (1.6  $\mu$ g) and loading control pRL-CMV luciferase reporter plasmid (20 ng) were transfected into P19 cells with the CMV-FoxA1 expression vector (200 ng) or a CMV empty expression vector (200 ng). Protein lysates were prepared at 24 h following transfection, and used to measure dual Luciferase enzyme activity.

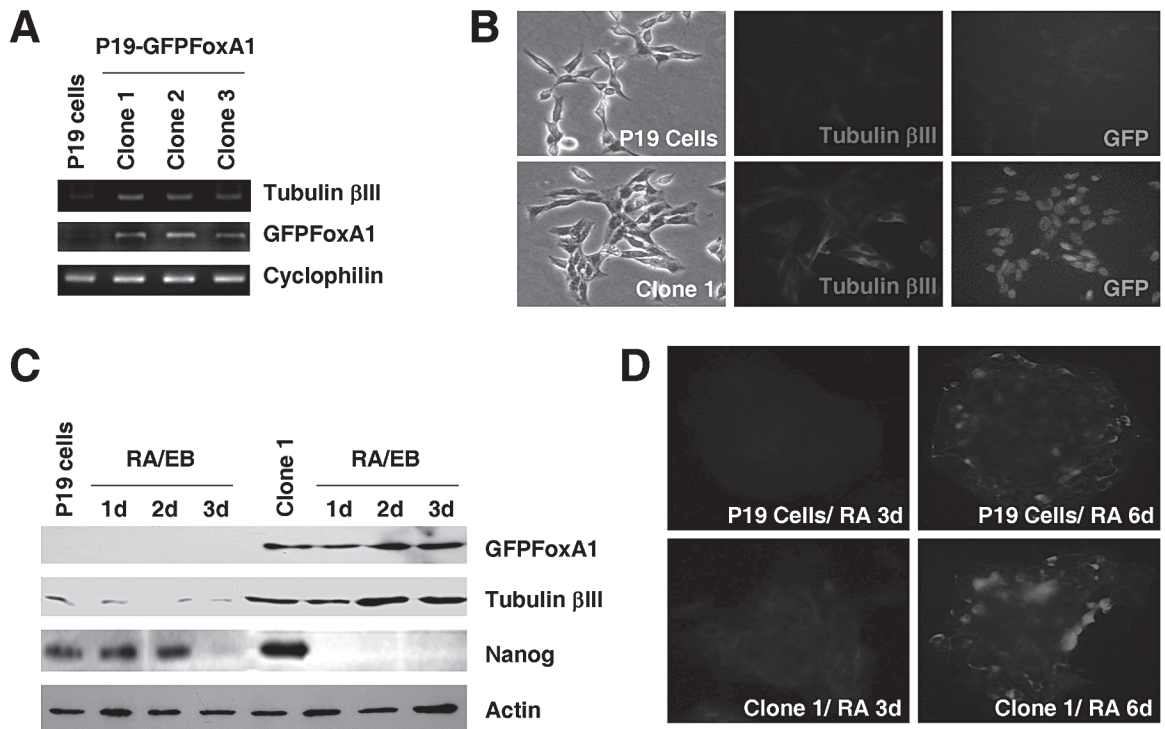


Figure 5. Increased expression of neuron-specific marker tubulin  $\beta$ III in P19 GFPFoxA1 cells, which show an earlier onset of neuronal differentiation through RA treatment. (A, B) P19 GFPFoxA1 cells express tubulin  $\beta$ III. Total RNA samples were isolated from P19 cells and clone 1, 2, and 3 of P19 GFPFoxA1 cells. The mRNA levels of tubulin  $\beta$ III, GFPFoxA1, and cyclophilin were measured by RT-PCR Assays (A). Immunostaining of P19 cells or the clone 1 cells was performed with tubulin  $\beta$ III antibody (B). (C, D) P19 GFPFoxA1 cells showed a more rapid change on the Nanog decrease and the tubulin  $\beta$ III increase during RA-induced neuronal differentiation. P19 cells and the clone 1 cells were treated with RA according to neural differentiation protocol. Total proteins samples were isolated and the protein levels of GFPFoxA1, tubulin  $\beta$ III, Nanog, and  $\beta$ -actin were measured by Western blotting (C). The differentiated cell samples induced by RA at day 3 or day 6 were immunostained with tubulin  $\beta$ III (D).

are required for maintenance of pluripotency of stem cells (4,22). The expression of Nanog disappeared between day 2 to day 3 during RA-induced P19 cell differentiation but its expression was undetectable as early as at day 1 of differentiated P19 GFPFoxA1 cells (Fig. 5C). Furthermore, we noticed that the tubulin  $\beta$ III expression was increased rapidly during differentiation in P19 GFPFoxA1 cells, even at day 2 post-RA treatment (Fig. 5C). The rapid elevation of tubulin  $\beta$ III expression during P19 GFPFoxA1 cell differentiation was confirmed by the immunostaining analysis, in which the day 3 samples of RA-induced P19 GFPFoxA1 cell showed obvious positive signals compared with the P19 cell controls (Fig. 5D). At the terminal differentiation phase (day 6 post-RA treatment) where the GFPFoxA1 fusion protein was still detectable in P19 GFPFoxA1 cells (Fig. 3S, B; supplement figures available from [http://bio.hnu.cn/index.php?option=com\\_content&view=article&id=131:2010-11-16-12-45-48&catid=46:2010-07-19-05-57-39&Itemid=123](http://bio.hnu.cn/index.php?option=com_content&view=article&id=131:2010-11-16-12-45-48&catid=46:2010-07-19-05-57-39&Itemid=123)), both differentiated P19 and P19 GFPFoxA1 cells expressed tubulin  $\beta$ III (Fig. 5D), suggesting that the neuronal populations were produced from the two cell types by RA. Together, the

data suggested that P19 GFPFoxA1 cells maintained the ability to produce neuronal cells and could be differentiated faster than their parental P19 cells.

FoxA1 is one of the major regulators that control P19 cell neuronal differentiation, evidenced by the change of its expression pattern post-RA treatment (10), the stimulation of its transcription by RA receptors (11), and its regulation on the Shh expression (34). In this study, we have established P19 cell-derived cell lines that stably express a GFP-FoxA1 fusion protein to further explore the biological roles of FoxA1 during neuronal differentiation. The P19 GFPFoxA1 cells show partial loss of pluripotency of P19 stem cells and several characteristics of neural stem cells, such as the decreased activity of alkaline phosphatase, the increased expression of SSEA-3, the elevated levels of nestin expression, and the increased populations of prominin-1<sup>+</sup> cells. These phenotypes could be explained partially by the FoxA1 direct stimulation on the promoter of nestin, which promotes pluripotent P19 cells to become neural stem-like cells. Interestingly, the pluripotency-related Oct4, Nanog, and Sox2 express normally in P19 GFPFoxA1 cells. Although these factors are



confirmed to play critical roles in pluripotent stem cells, there are evidences showing that neural stem cells also express Oct4, Nanog, and Sox2 (6,16,25). Furthermore, P19 GFPFoxA1 cells show an earlier onset of differentiation during RA-induced neuronal differentiation, evidenced by a more rapid decrease of Nanog and increase of tubulin  $\beta$ III. Our findings suggest that FoxA1 is one of the major factors, which stimulate the transition from pluripotent stem cell stage to neural stem cell stage during RA-induced P19 cell neuronal differentiation.

We also found that P19 GFPFoxA1 cells maintained the ability to produce neuronal cells at the terminal differentiation phase post-RA treatment. At least within in vitro neuronal differentiation conditions, P19 GFPFoxA1 cells were showed to differentiate faster than their parental P19 cells. This could be caused by the existence of partial characteristics of neural stem cells and the tubulin  $\beta$ III expression

in P19 GFPFoxA1 cells. P19 GFPFoxA1 cells provide us suitable experimental materials to trace the differentiation progression in vivo because they are GFP-labeled cells. In the future, the cells allow us to test whether the FoxA1 stable expression in pluripotent P19 cells improves the production of neuronal cells within in vivo models.

#### ACKNOWLEDGMENTS

This work was supported by Natural Science Foundation of China (grant numbers 30771096, 30871244 to Y.T.) and the Ministry of Science and Technology of China (grant number 2010DFB30300). All the supplement figures can be accessed at: [http://bio.hnu.cn/index.php?option=com\\_content&view=article&id=131:2010-11-16-12-45-48&catid=46:2010-07-19-05-57-39&Itemid=123](http://bio.hnu.cn/index.php?option=com_content&view=article&id=131:2010-11-16-12-45-48&catid=46:2010-07-19-05-57-39&Itemid=123)

#### REFERENCES

- Andrews, P. W. Human teratocarcinoma stem cells: Glycolipid antigen expression and modulation during differentiation. *J. Cell Biochem.* 35:321–332; 1987.
- Ang, S. L.; Wierda, A.; Wong, D.; Stevens, K. A.; Cascio, S.; Rossant, J.; Zaret, K. S. The formation and maintenance of the definitive endoderm lineage in the mouse: Involvement of HNF3/forkhead proteins. *Development* 119:1301–1315; 1993.
- Besnard, V.; Wert, S. E.; Hull, W. M.; Whitsett, J. A. Immunohistochemical localization of Foxa1 and Foxa2 in mouse embryos and adult tissues. *Gene Expression Patterns* 5:193–208; 2004.
- Chambers, I.; Colby, D.; Robertson, M.; Nichols, J.; Lee, S.; Tweedie, S.; Smith, A. Functional expression cloning of Nanog, a pluripotency sustaining factor in embryonic stem cells. *Cell* 113:643–655; 2003.
- Damjanov, I.; Fox, N.; Knowles, B. B.; Solter, D.; Lange, P. H.; Fraley, E. E. Immunohistochemical localization of murine stage-specific embryonic antigens in human testicular germ cell tumors. *Am. J. Pathol.* 108:225–230; 1982.
- Du, Z.; Jia, D.; Liu, S.; Wang, F.; Li, G.; Zhang, Y.; Cao, X.; Ling, E. A.; Hao, A. Oct4 is expressed in human gliomas and promotes colony formation in glioma cells. *Glia* 57:724–733; 2009.
- Edwards, M. K.; Harris, J. F.; McBurney, M. W. Induced muscle differentiation in an embryonal carcinoma cell line. *Mol. Cell. Biol.* 3:2280–2286; 1983.
- Ferri, A. L. M.; Lin, W.; Mavromatakis, Y. E.; Wang, J. C.; Sasaki, H.; Whitsett, J. A.; Ang, S.-L. Foxa1 and Foxa2 regulate multiple phases of midbrain dopaminergic neuron development in a dosage-dependent manner. *Development* 134:2761–2769; 2007.
- Friedman, J. R.; Kaestner, K. H. The Foxa family of transcription factors in development and metabolism. *Cell. Mol. Life Sci.* 63:2317–2328; 2006.
- Jacob, A.; Budhiraja, S.; Reichel, R. R. Differential induction of HNF-3 transcription factors during neuronal differentiation. *Exp. Cell Res.* 234:277–284; 1997.
- Jacob, A.; Budhiraja, S.; Reichel, R. R. The HNF-3[alpha] transcription factor is a primary target for retinoic acid action. *Exp. Cell Res.* 250:1–9; 1999.
- Jones-Villeneuve, E. M.; McBurney, M. W.; Rogers, K. A.; Kalnins, V. I. Retinoic acid induces embryonal carcinoma cells to differentiate into neurons and glial cells. *J. Cell. Biol.* 94:253–262; 1982.
- Kaestner, K. H.; Knochel, W.; Martinez, D. E. Unified nomenclature for the winged helix/forkhead transcription factors. *Genes Dev.* 14:142–146; 2000.
- Kaufmann, E.; Knochel, W. Five years on the wings of fork head. *Mech. Dev.* 57:3–20; 1996.
- Lee, M. S.; Jun, D. H.; Hwang, C. I.; Park, S. S.; Kang, J. J.; Park, H. S.; Kim, J.; Kim, J. H.; Seo, J. S.; Park, W. Y. Selection of neural differentiation-specific genes by comparing profiles of random differentiation. *Stem Cells* 24:1946–1955; 2006.
- Lee, S. H.; Jeyapalan, J. N.; Appleby, V.; Mohamed Noor, D. A.; Sottile, V.; Scotting, P. J. Dynamic methylation and expression of Oct4 in early neural stem cells. *J. Anat.* 217:203–213; 2010.
- Lehmann, O. J.; Sowden, J. C.; Carlsson, P.; Jordan, T.; Bhattacharya, S. S. Fox's in development and disease. *Trends Genet.* 19:339–344; 2003.
- Lendahl, U.; Zimmerman, L. B.; McKay, R. D. CNS stem cells express a new class of intermediate filament protein. *Cell* 60:585–595; 1990.
- Martin, G. Teratocarcinomas and mammalian embryogenesis. *Science* 209:768–776; 1980.
- McBurney, M. W.; Jones-Villeneuve, E. M.; Edwards, M. K.; Anderson, P. J. Control of muscle and neuronal differentiation in a cultured embryonal carcinoma cell line. *Nature* 299:165–167; 1982.
- McBurney, M. W.; Rogers, B. J. Isolation of male

- embryonal carcinoma cells and their chromosome replication patterns. *Dev. Biol.* 89:503–508; 1982.
22. Mitsui, K.; Tokuzawa, Y.; Itoh, H.; Segawa, K.; Murakami, M.; Takahashi, K.; Maruyama, M.; Maeda, M.; Yamanaka, S. The homeoprotein Nanog is required for maintenance of pluripotency in mouse epiblast and ES cells. *Cell* 113:631–642; 2003.
  23. Monaghan, A. P.; Kaestner, K. H.; Grau, E.; Schutz, G. Postimplantation expression patterns indicate a role for the mouse forkhead/HNF-3 a, b and g genes in determination of the definitive endoderm, chordamesoderm and neuroectoderm. *Development* 119:567–578; 1993.
  24. Pevny, L. H.; Sockanathan, S.; Placzek, M.; Lovell-Badge, R. A role for SOX1 in neural determination. *Development* 125:1967–1978; 1998.
  25. Po, A.; Ferretti, E.; Miele, E.; De Smaele, E.; Paganelli, A.; Canettieri, G.; Coni, S.; Di Marcotullio, L.; Biffoni, M.; Massimi, L.; Di Rocco, C.; Screpanti, I.; Gulino, A. Hedgehog controls neural stem cells through p53-independent regulation of Nanog. *EMBO J.* 29:2646–2658; 2010.
  26. Pruitt, S. C. Discrete endogenous signals mediate neural competence and induction in P19 embryonal carcinoma stem cells. *Development* 120:3301–3312; 1994.
  27. Rausa, F. M.; Tan, Y.; Costa, R. H. Association between hepatocyte nuclear factor 6 (HNF-6) and FoxA2 DNA binding domains stimulates FoxA2 transcriptional activity but inhibits HNF-6 DNA binding. *Mol. Cell. Biol.* 23:437–449; 2003.
  28. Rossant, J.; McBurney, M. W. The developmental potential of a euploid male teratocarcinoma cell line after blastocyst injection. *J. Embryol. Exp. Morphol.* 70:99–112; 1982.
  29. Ruiz i Altaba, A.; Prezioso, V. R.; Darnell, J. E.; Jessell, T. M. Sequential expression of HNF-3b and HNF-3a by embryonic organizing centers: The dorsal lip/node, notochord and floor plate. *Mech. Dev.* 44: 91–108; 1993.
  30. Sasaki, H.; Hogan, B. L. Differential expression of multiple fork head related genes during gastrulation and axial pattern formation in the mouse embryo. *Development* 118:47–59; 1993.
  31. Schwob, A. E.; Nguyen, L. J.; Meiri, K. F. Immortalization of neural precursors when telomerase is overexpressed in embryonal carcinomas and stem cells. *Mol. Biol. Cell* 19:1548–1560; 2008.
  32. Tan, Y.; Costa, R. H.; Kovessi, I.; Reichel, R. R. Adenovirus-mediated increase of HNF-3 levels stimulates expression of transthyretin and sonic hedgehog, which is associated with F9 cell differentiation toward the visceral endoderm lineage. *Gene Expr.* 9:237–248; 2001.
  33. Tan, Y.; Raychaudhuri, P.; Costa, R. H. Chk2 mediates stabilization of the FoxM1 transcription factor to stimulate expression of DNA repair genes. *Mol. Cell. Biol.* 27:1007–1016; 2007.
  34. Tan, Y.; Xie, Z.; Ding, M.; Wang, Z.; Yu, Q.; Meng, L.; Zhu, H.; Huang, X.; Yu, L.; Meng, X.; Chen, Y. Increased levels of FoxA1 transcription factor in pluripotent P19 embryonal carcinoma cells stimulate neural differentiation. *Stem Cells Dev* 19:1365–1374; 2009.
  35. Varga, B.; Hadinger, N.; Gocza, E.; Dulberg, V.; Demeter, K.; Madarasz, E.; Herberth, B. Generation of diverse neuronal subtypes in cloned populations of stem-like cells. *BMC Dev. Biol.* 8:89; 2008.
  36. Xia, C.; Wang, C.; Zhang, K.; Qian, C.; Jing, N. Induction of a high population of neural stem cells with anterior neuroectoderm characters from epiblast-like P19 embryonic carcinoma cells. *Differentiation* 75: 912–927; 2007.
  37. Xie, Z.; Tan, G.; Ding, M.; Dong, D.; Chen, T.; Meng, X.; Huang, X.; Tan, Y. Foxm1 transcription factor is required for maintenance of pluripotency of P19 embryonal carcinoma cells. *Nucleic Acids Res.* 38(22): 8027–8038; 2010.
  38. Yu, J.; Thomson, J. A. Pluripotent stem cell lines. *Genes Dev.* 22:1987–1997; 2008.